

## Supporting Information

### Synthesis of amine-bridged bis(phenolate) rare-earth metal aryloxides and their catalytic performances for the ring-opening polymerization of $L$ -lactic acid $O$ -carboxyanhydride and $L$ -lactide

Hao Ouyang,<sup>a</sup> Kun Nie,<sup>\*a,b</sup> Dan Yuan,<sup>a</sup> and Yingming Yao<sup>\*,a,c</sup>

*<sup>a</sup>Key Laboratory of Organic Synthesis of Jiangsu Province, and State and Local Joint Engineering Laboratory for Novel Functional Polymeric Materials, College of Chemistry, Chemical Engineering and Materials Science, Dushu Lake Campus, Soochow University, Suzhou 215123, People's Republic of China*

*<sup>b</sup>School of Chemistry and Chemical Engineering, Taishan University, Taian 271021, People's Republic of China*

*<sup>c</sup>State Key Laboratory of Polymer Physics and Chemistry, Changchun Institute of Applied Chemistry, Chinese Academy of Sciences, Changchun 130022, People's Republic of China*

\* To whom correspondence should be addressed. Email: yaoym@suda.edu.cn (Y.

Yao)

# Contents

- Fig. S1**  $^1\text{H}$  NMR spectrum ( $\text{CDCl}_3$ , 25 °C) of  ${}_L$ -lacOCA
- Fig. S2**  $^{13}\text{C}$  NMR spectrum ( $\text{CDCl}_3$ , 25 °C) of  ${}_L$ -lacOCA
- Fig. S3**  $^1\text{H}$  NMR spectrum (DMSO, 25 °C) of complex **1**
- Fig. S4**  $^{13}\text{C}$  NMR spectrum (DMSO, 25 °C) of complex **1**
- Fig. S5**  $^1\text{H}$  NMR spectrum ( $\text{C}_6\text{D}_6$ , 25 °C) of complex **2**
- Fig. S6**  $^{13}\text{C}$  NMR spectrum ( $\text{C}_6\text{D}_6$ , 25 °C) of complex **2**
- Fig. S7**  $^1\text{H}$  NMR spectrum ( $\text{C}_6\text{D}_6$ , 25 °C) of complex **3**
- Fig. S8**  $^{13}\text{C}$  NMR spectrum ( $\text{C}_6\text{D}_6$ , 25 °C) of complex **3**
- Fig. S9**  $^1\text{H}$  NMR spectrum ( $d_8$ -THF, 25 °C) of complex **5**
- Fig. S10**  $^{13}\text{C}$  NMR spectrum ( $d_8$ -THF, 25 °C) of complex **5**
- Table S1.** Crystallographic data for complexes **1**, **2**, **3** and **5**
- Table S2.** Selected bond lengths (Å) and bond angles (deg) for complexes **1-5**
- Fig. S11** Solid state structure of **2**.
- Fig. S12** Plot of PLA Mn(■) and polydispersity (▲) as a function of  ${}_L$ -lacOCA conversion initiated by complex **5**
- Fig. S13**  $^1\text{H}$  NMR (normal) spectrum of PLLA obtained from  ${}_L$ -lacOCA.
- Fig. S14**  $^{13}\text{C}$  NMR spectrum of PLLA obtained from  ${}_L$ -lacOCA
- Fig. S15**  $^1\text{H}$  NMR (homodecoupled) spectrum of PLLA obtained from  ${}_L$ -lacOCA
- Fig. S16** DSC thermogram of poly(lactic acid)
- Fig. S17** TGA thermogram of poly(lactic acid)

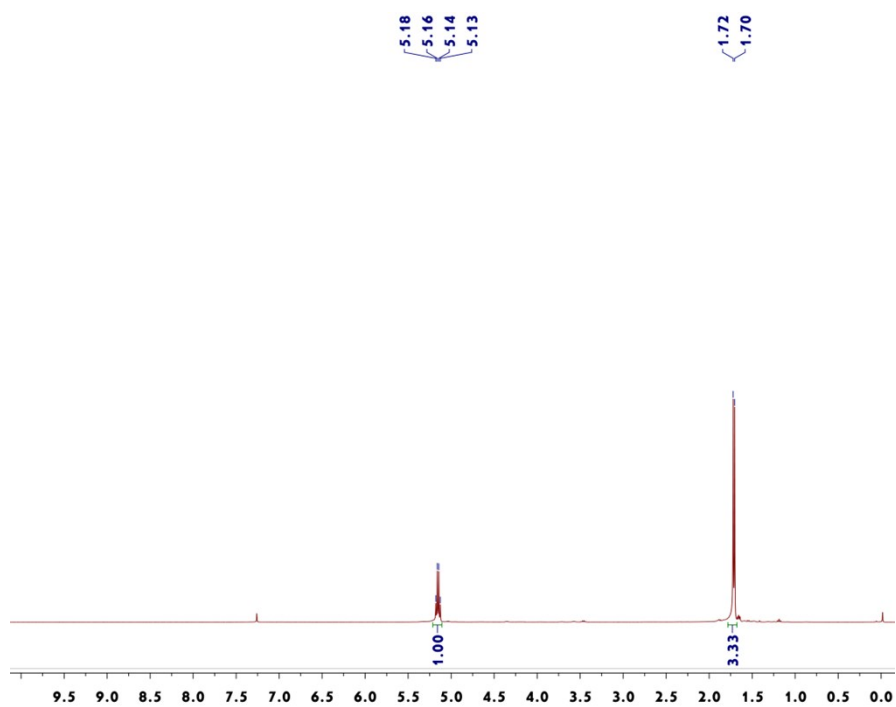


**Fig. S1**  $^1\text{H}$  NMR spectrum ( $\text{CDCl}_3$ , 25  $^\circ\text{C}$ ) of  $\text{L-lacOCA}$

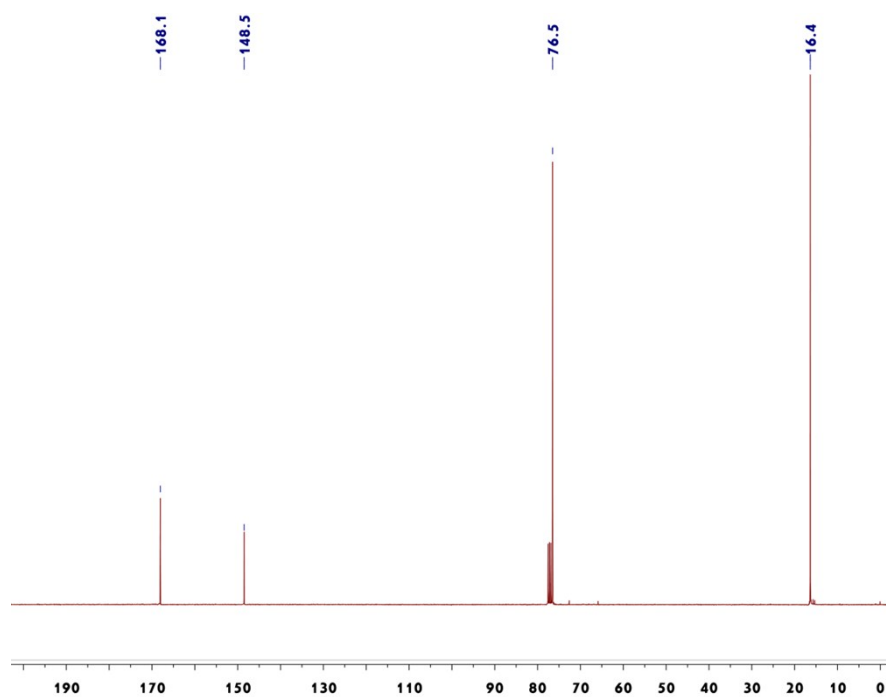


**Fig. S2**  $^{13}\text{C}$  NMR spectrum ( $\text{CDCl}_3$ , 25  $^\circ\text{C}$ ) of  $\text{L-lacOCA}$

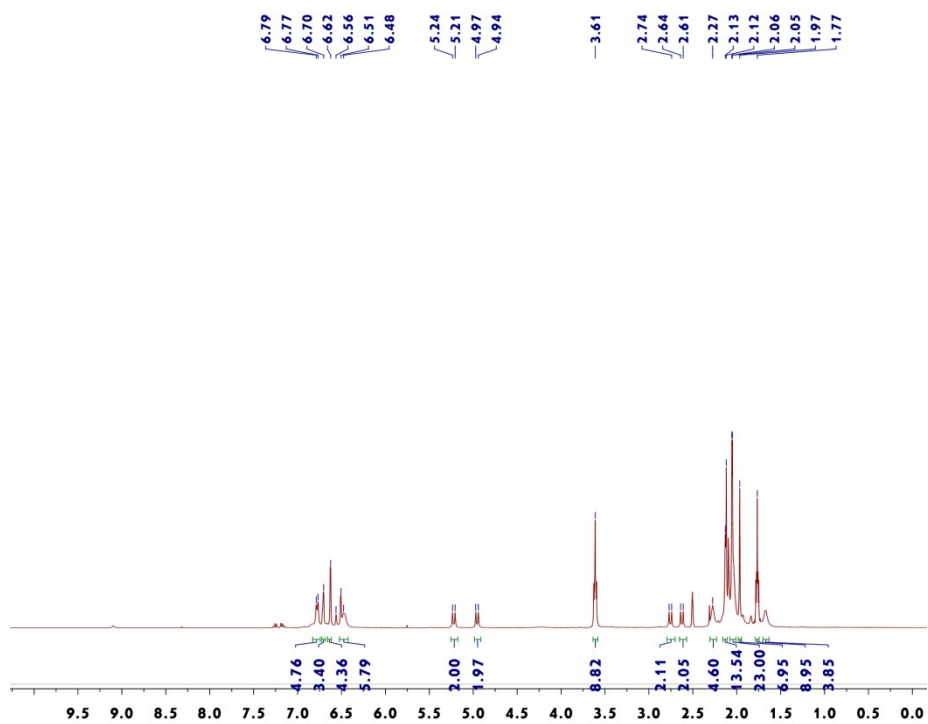


**Fig. S3**  $^1\text{H}$  NMR spectrum (DMSO, 25 °C) of complex **1**

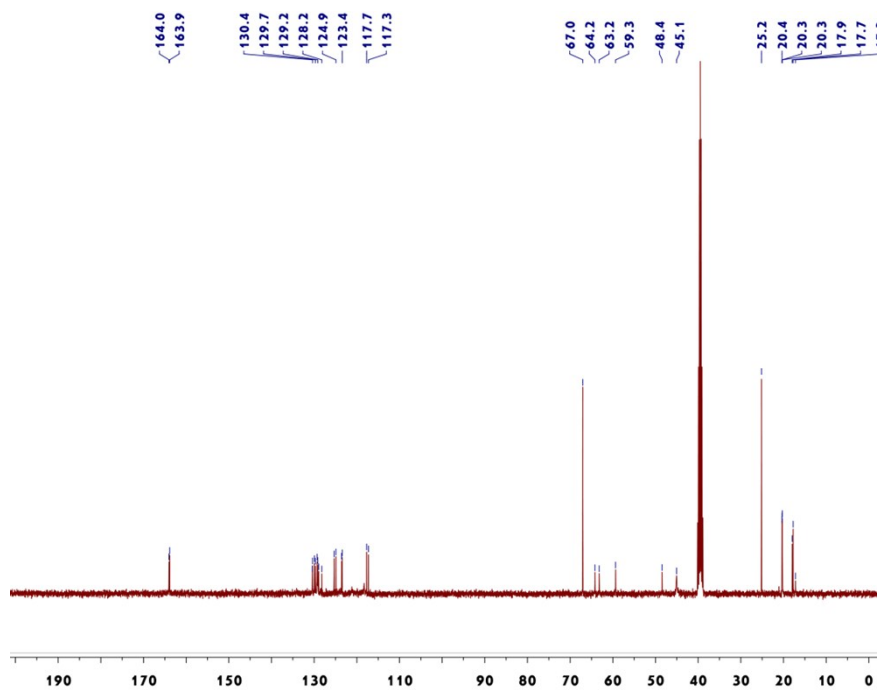


**Fig. S4**  $^{13}\text{C}$  NMR spectrum (DMSO, 25 °C) of complex **1**

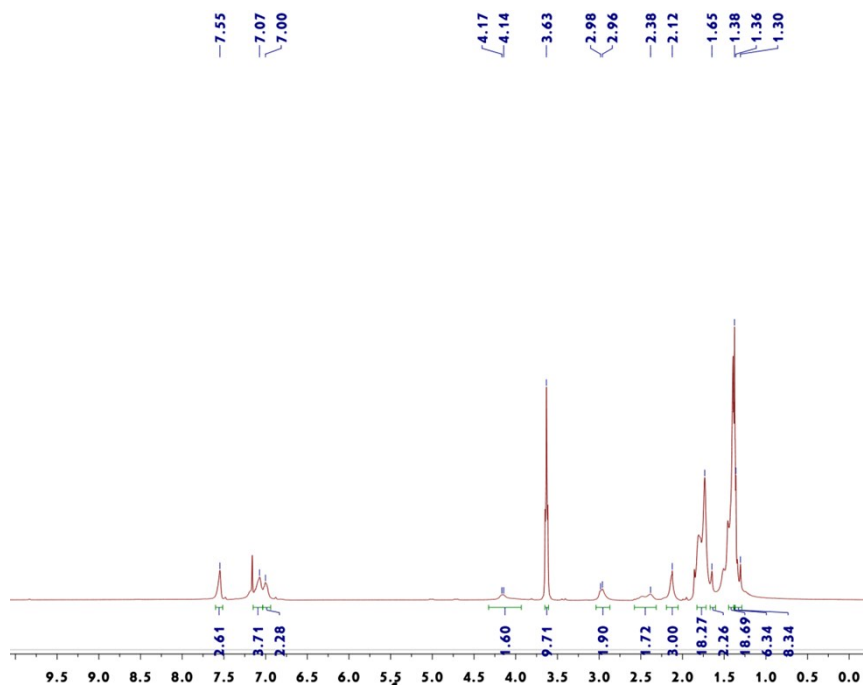


Fig. S5  $^1\text{H}$  NMR spectrum ( $\text{C}_6\text{D}_6$ , 25 °C) of complex 2

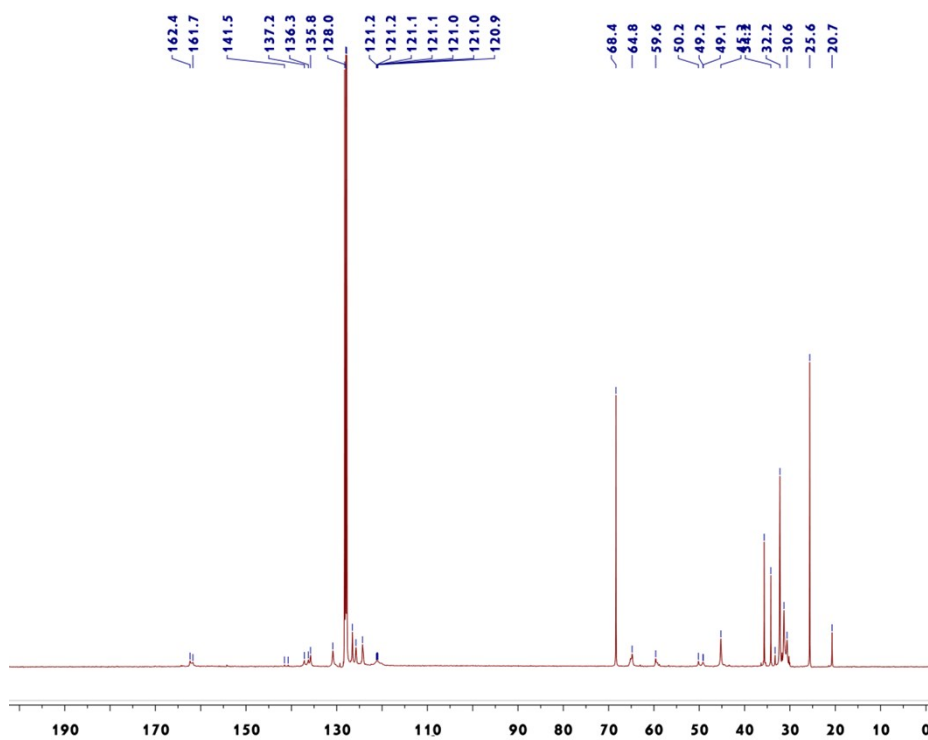


Fig. S6  $^{13}\text{C}$  NMR spectrum ( $\text{C}_6\text{D}_6$ , 25 °C) of complex 2

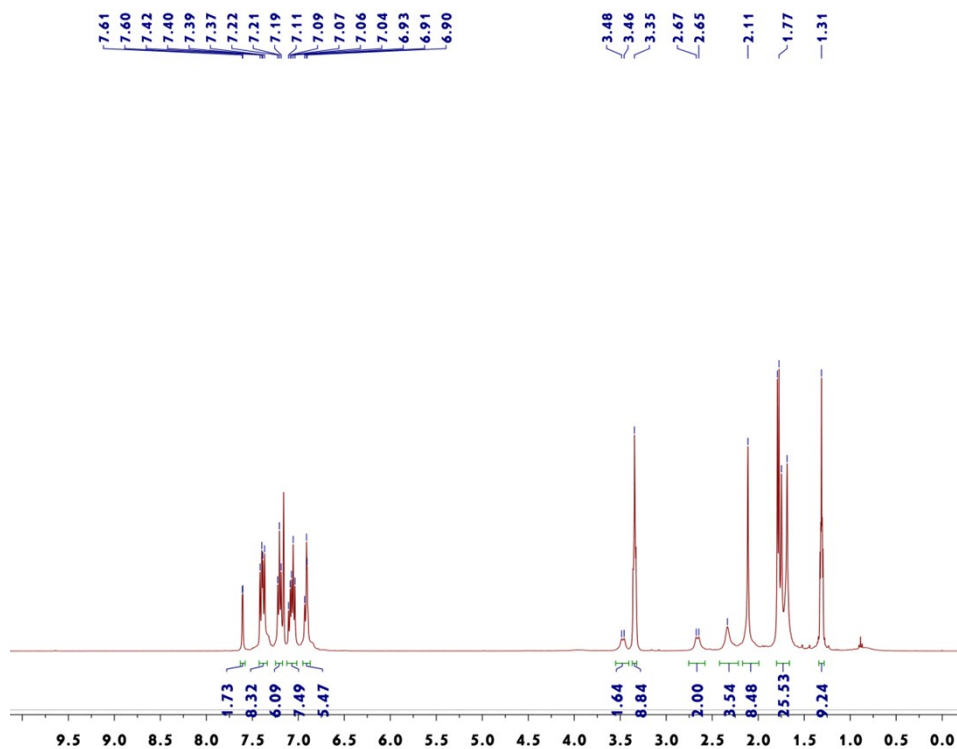


Fig. S7  $^1\text{H}$  NMR spectrum ( $\text{C}_6\text{D}_6$ , 25  $^\circ\text{C}$ ) of complex **3**

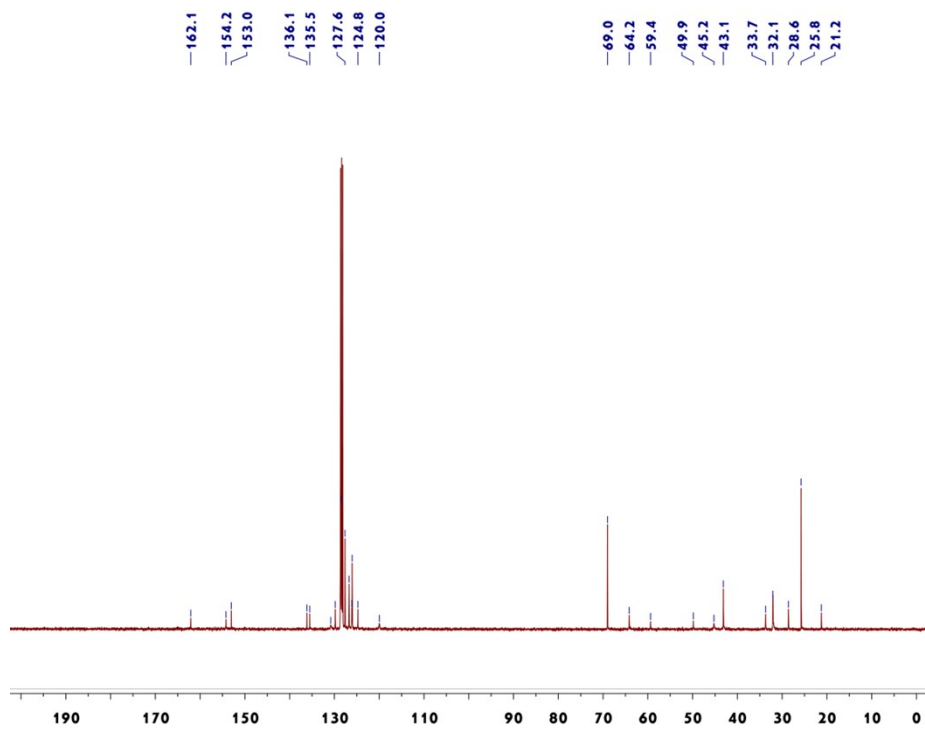
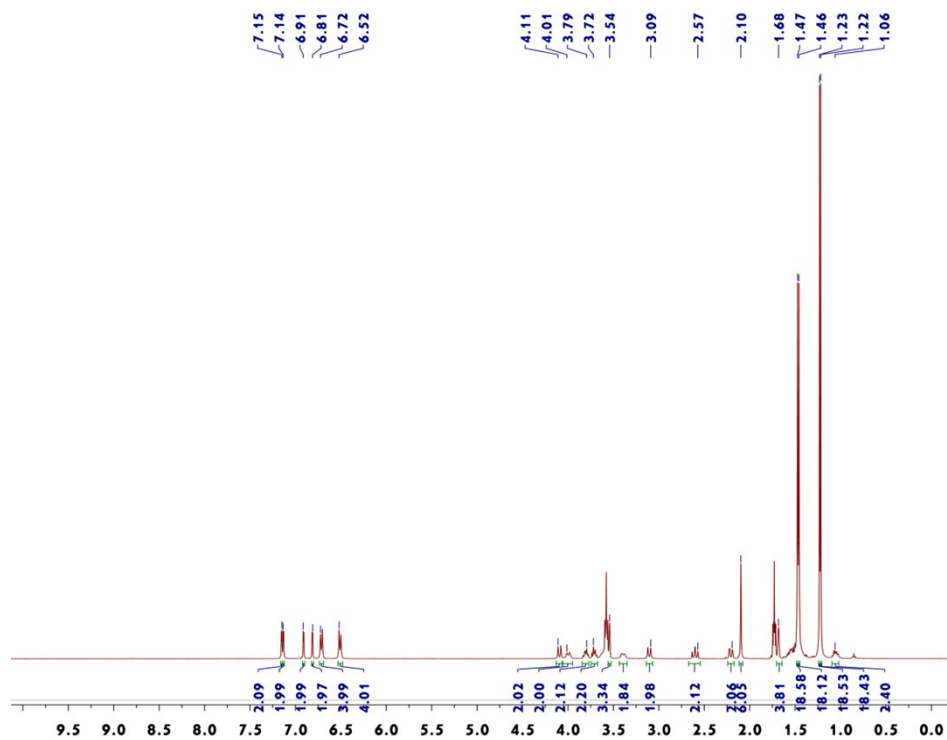
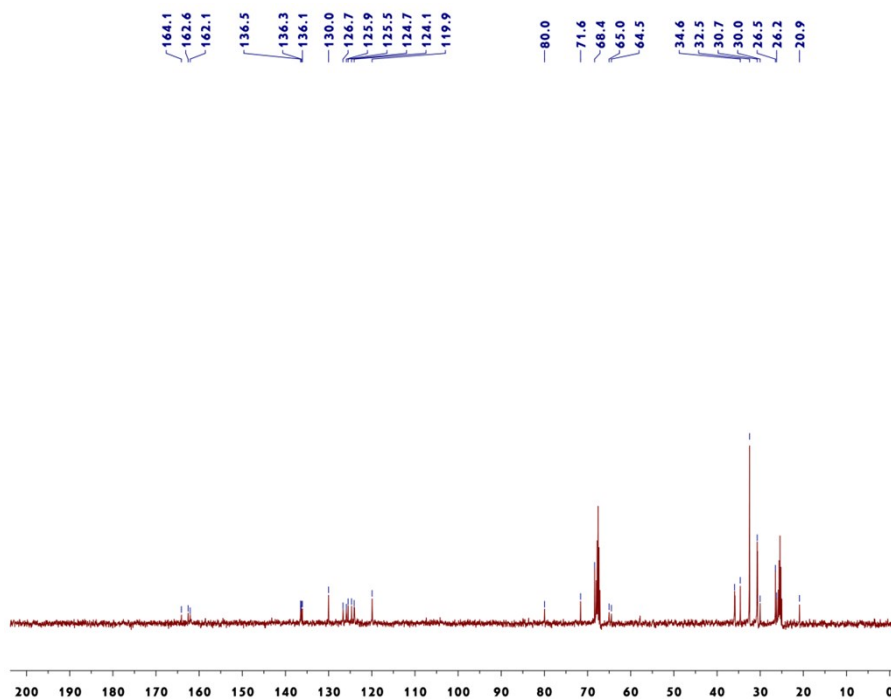


Fig. S8  $^{13}\text{C}$  NMR spectrum ( $\text{C}_6\text{D}_6$ , 25  $^\circ\text{C}$ ) of complex **3**



**Fig. S9**  $^1\text{H}$  NMR spectrum ( $d_8$ -THF, 25 °C) of complex **5**



**Fig. S10**  $^{13}\text{C}$  NMR spectrum ( $d_8$ -THF, 25 °C) of complex **5**

**Table S1.** Crystallographic data for complexes **1**, **2**, **3** and **5**

Compound	<b>1</b>	<b>2</b>	<b>3</b>	<b>5·3THF</b>
Formula	C <sub>74</sub> H <sub>106</sub> La <sub>2</sub> N <sub>4</sub> O <sub>10</sub>	C <sub>49</sub> H <sub>77</sub> N <sub>2</sub> O <sub>5</sub> L a	C <sub>69</sub> H <sub>85</sub> LaN <sub>2</sub> O <sub>5</sub>	C <sub>180</sub> H <sub>264</sub> N <sub>4</sub> O <sub>19</sub> Y <sub>4</sub>
fw	1489.45	913.03	1161.29	3143.58
<i>T</i> /K	293(2)	100(2)	293(2)	223(2)
Crystal system	triclinic	orthorhombic	monoclinic	triclinic
Crystal size/mm	0.60 x 0.40 x 0.20	0.35 × 0.30 × 0.20	0.75 x 0.6 x 0.4	0.80 x 0.70 x 0.30
Space group	P-1	Pnma	P 1	P-1
<i>a</i> /Å	12.4210(6)	21.8235(10)	15.1660(3)	15.5796(11)
<i>b</i> /Å	12.9473(5)	20.4867(8)	33.8032(8)	18.2982(14)
<i>c</i> /Å	13.3644(7)	10.6023(5)	24.5524(6)	18.7574(18)
<i>α</i> /deg	114.347(4)	90	90	75.610(15)
<i>β</i> /deg	109.435(5)	90	101.496(2)	70.403(14)
<i>γ</i> /deg	95.310(4)	90	90	66.585(13)
<i>V</i> /Å <sup>3</sup>	1779.31(16)	4740.2(4)	12334.6(5)	4581.5(9)
<i>Z</i>	1	4	8	1
<i>D</i> <sub>calcd</sub> /g cm <sup>-3</sup>	1.390	1.279	1.251	1.139
<i>μ</i> /mm <sup>-1</sup>	1.243	0.946	0.743	1.312
<i>F</i> (000)	772	1928	4880	1680
<i>θ</i> <sub>max</sub> /deg	26.37	27.51	26.37	26.37
Collected	17526	42156	74083	40070
Unique reflns	7289	5581	25165	18548
Obsd reflns [ <i>I</i> > 2.0σ( <i>I</i> )]	6495	4642	19002	11014
No. of variables	371	295	1471	951
GOF	1.052	1.072	1.060	1.071
<i>R</i>	0.0368	0.0266	0.0447	0.0804
w <i>R</i>	0.0875	0.0553	0.0936	0.2251
<i>R</i> <sub>int</sub>	0.0316	0.0508	0.0414	0.0675
Largest diff. peak, hole/e Å <sup>-3</sup>	1.573,- 1.712	0.875, -0.399	0.962,- 0.755	1.480, - 1.358



**Table S2.** Selected bond lengths (Å) and bond angles (deg) for complexes **1-3 and 5**.

<b>Bond lengths</b>	<b>1</b>	<b>Bond lengths</b>	<b>2</b>
Ln1-O1	2.465(2)	Ln1-O1	2.285(13)
Ln1-O1A	2.435(2)	Ln1-O1A	2.285(13)
Ln1-O2	2.313(2)	Ln1-O2	2.284(2)
Ln1-O3	2.289(3)	Ln1-O3	2.608(2)
Ln1-O4	2.682(3)	Ln1-O4	2.646(2)
Ln1-N1	2.848(3)	Ln1-N1	2.754(2)
Ln1-N2	2.730(3)	Ln1-N2	2.755(3)
<b>Bond angles</b>		<b>Bond angles</b>	
O2-Ln1-N1	71.20(8)	O1-Ln1-O2	106.74(4)
N2-Ln1-N1	63.97(9)	O2-Ln1-O1A	106.74(3)
O1A-Ln1-N1	106.15(8)	O1-Ln1-O1A	145.52(7)
O3-Ln1-N1	131.12(9)	O2-Ln1-N1	140.88(8)
O3-Ln1-O1	86.79(9)	O1-Ln1-N1	74.48(4)
O3-Ln1-O2	138.69(10)	O2-Ln1-N2	76.84(8)
O3-Ln1-O1A	105.72(9)	O1-Ln1-N2	89.85(4)
O2-Ln1-O1A	97.01(8)	N1-Ln1-N2	64.04(7)
O1A-Ln1-O1	67.67(8)		

<b>Bond lengths</b>	<b>3</b>	<b>Bond lengths</b>	<b>5</b>
Ln1-O1	2.301(2)	Ln1-O1	2.136(4)
Ln1-O2	2.269(2)	Ln1-O2	2.128(4)
Ln1-O3	2.270(3)	Ln1-O3	2.339(4)
Ln1-O4	2.679(3)	Ln1-O3A	2.263(4)
Ln1-O5	2.619(3)	Ln1-O4	2.365(4)
Ln1-N1	2.783(2)	Ln1-N1	2.542(5)
Ln1-N2	2.809(3)		
<b>Bond angles</b>		<b>Bond angles</b>	
O2-Ln1-N1	74.26(7)	O2-Ln1-N1	76.66(15)
N1-Ln1-N2	63.46(8)	O3-Ln1-N1	127.13(14)
O3-Ln1-N1	139.95(9)	O3A-Ln1-N1	163.70(15)
O4-Ln1-N1	77.43(8)	O4-Ln1-N1	67.47(14)
O1-Ln1-O3	111.44(10)	O2-Ln1-O3	100.19(14)
O1-Ln1-O4	84.00(8)	O2-Ln1-O3A	104.36(14)
O3-Ln1-O4	141.24(9)	O3-Ln1-O3A	69.02(15)
O4-Ln1-O5	68.92(9)	O4-Ln1-O3A	119.38(14)

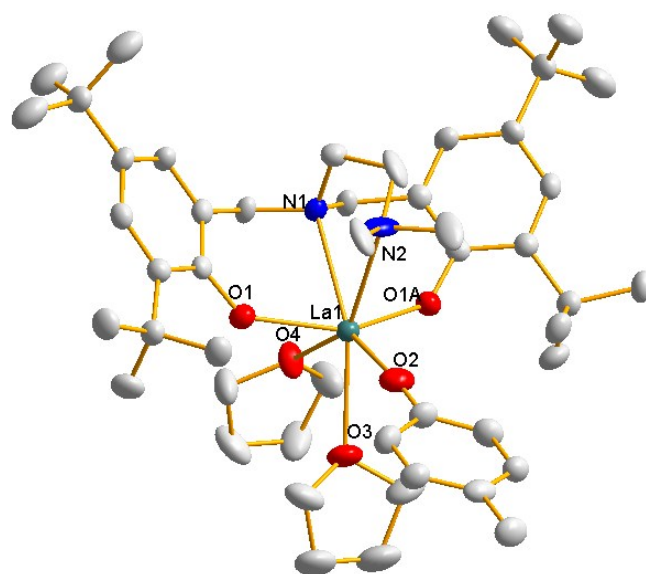


**Fig. S11** Solid state structure of complex **2** showing an atom numbering scheme. Thermal ellipsoids are drawn at 30% probability level, and hydrogen atoms are omitted for clarity.

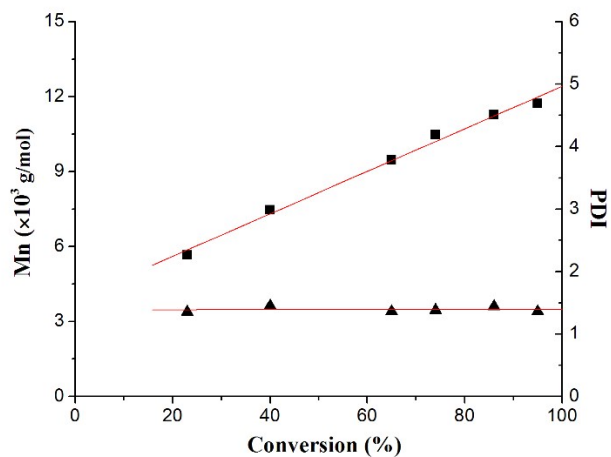


**Fig. S12** Plot of PLA Mn(■) and polydispersity (▲) as a function of  $L$ -lacOCA conversion initiated by complex **5**,  $[OCA]_0/[I]_0=200:1$ ,  $T=30\text{ }^\circ\text{C}$ .

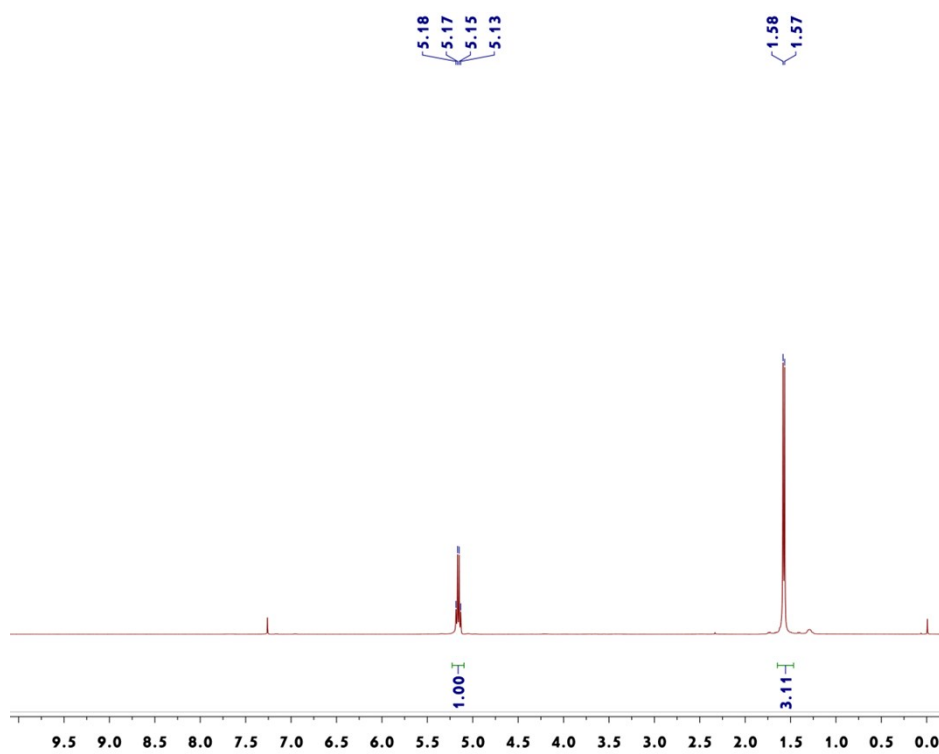


**Fig. S13**  $^1\text{H}$  NMR (normal) spectrum of PLLA obtained from  $L$ -lacOCA by complex **5**.

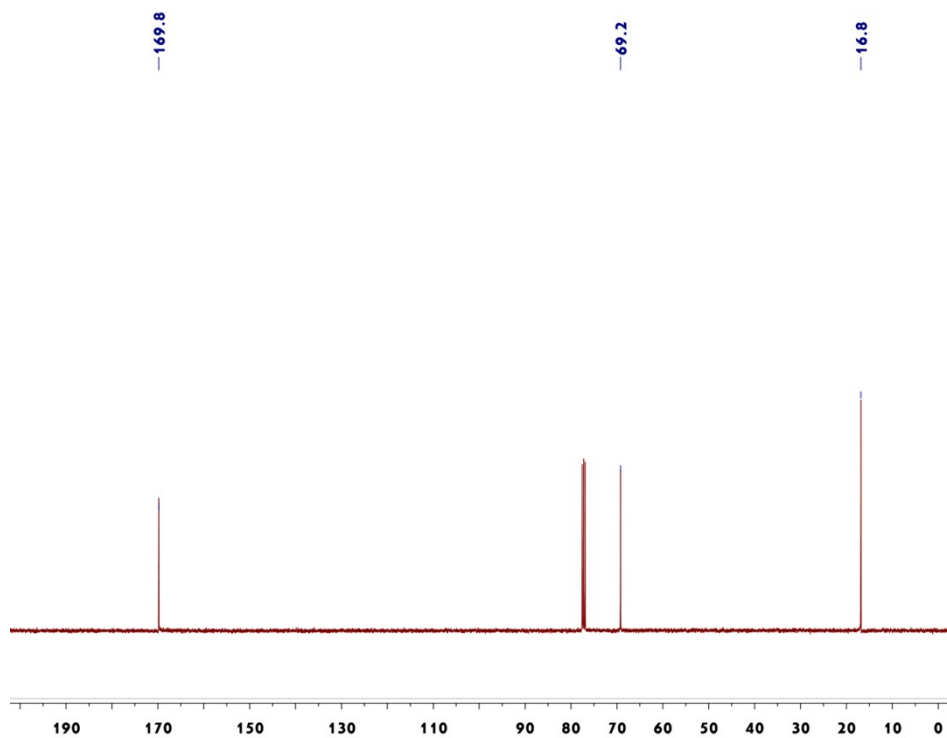


**Fig. S14**  $^{13}\text{C}$  NMR spectrum of PLLA obtained from  $L$ -lacOCA

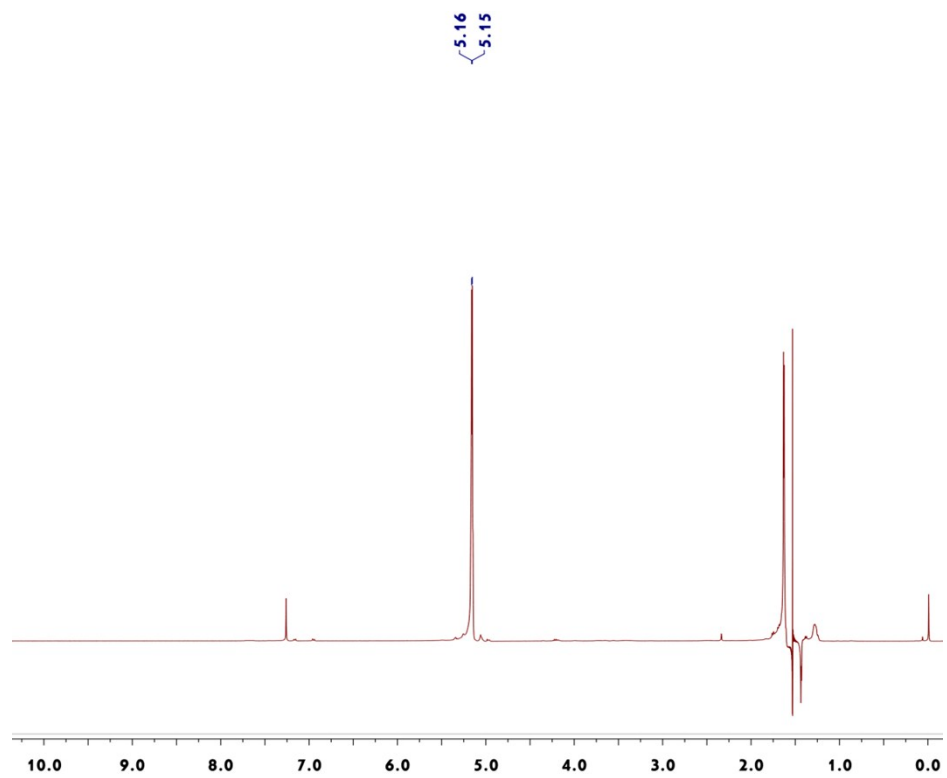


**Fig. S15**  $^1\text{H}$  NMR (homodecoupled) spectrum of PLLA obtained from  $L$ -lacOCA

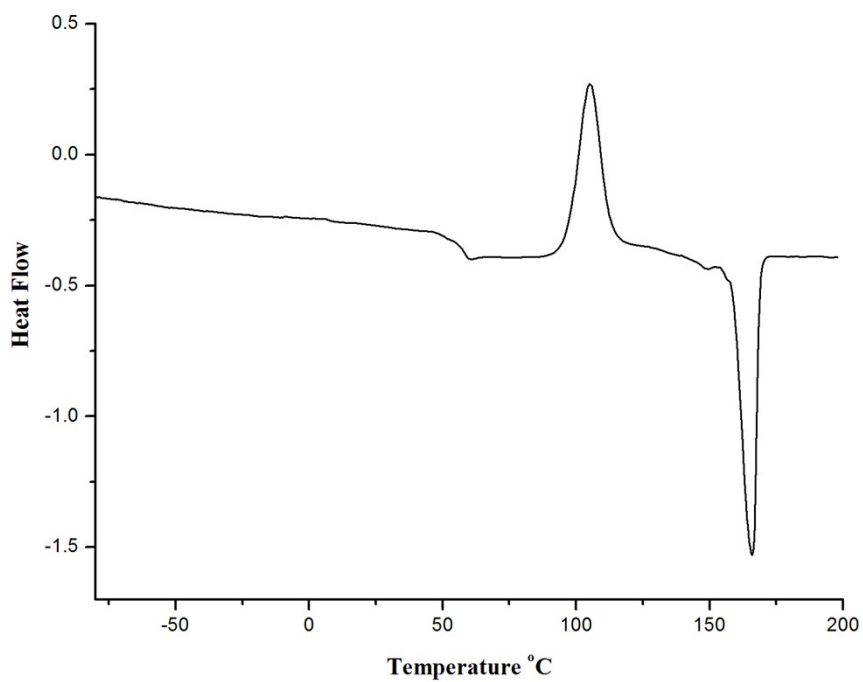


**Fig. S16** DSC thermogram of poly(lactic acid)

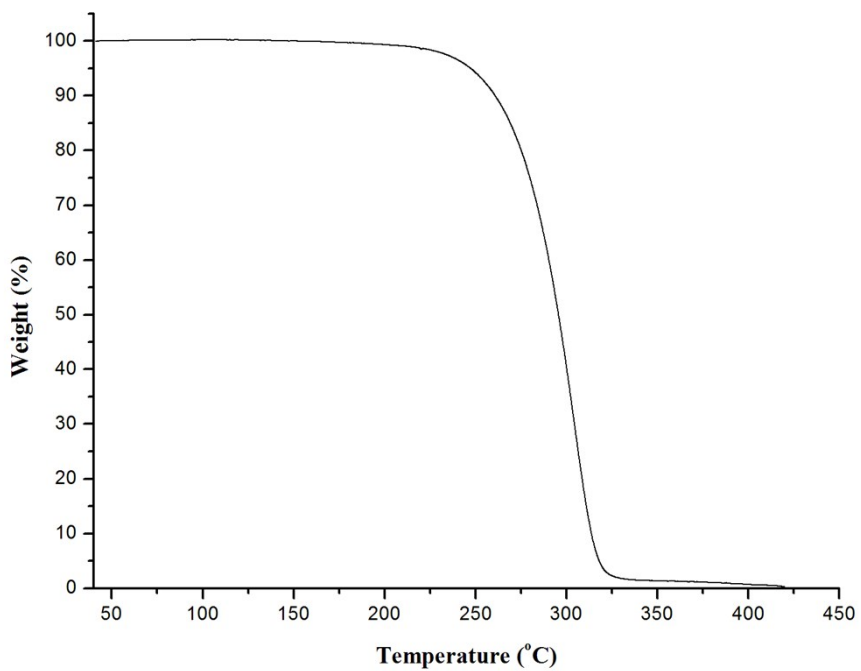


**Fig. S17** TGA thermogram of poly(lactic acid)